

Dynamical nuclear polarization and nuclear magnetic fields in semiconductor nanostructures

Ionel Tifrea* and Michael E. Flatté

Department of Physics and Astronomy and Optical Science and Technology Center, University of Iowa, Iowa City 52242, USA

(Dated: February 8, 2020)

We investigate the dynamic nuclear polarization from the hyperfine interaction between nonequilibrium electronic spins and nuclear spins coupled to them in semiconductor nanostructures. We derive the time and position dependence of the induced nuclear spin polarization and dipolar magnetic fields. In GaAs/AlGaAs parabolic quantum wells the nuclear spin polarization can be as high as 80% and the induced nuclear magnetic fields can approach a few gauss with an associated nuclear resonance shift of the order of kHz when the electronic system is 100% spin polarized. These fields and shifts can be tuned using small electric fields. We discuss the implications of such control for optical nuclear magnetic resonance experiments in low-dimensional semiconductor nanostructures.

PACS numbers: 76.60.-k, 76.70.Hb, 76.60.Cq

I. INTRODUCTION

Coherent control of the spin degrees of freedom in low dimensional semiconductor structures may lead to spin based electronic devices and quantum information processing^{1,2}. The practical realization of quantum computing requires the preparation, manipulation, and measurement of pure quantum states^{3–5}. Nuclear spins are ideal candidates, as all required conditions can be achieved based on the hyperfine interaction between electronic and nuclear spins^{5,6}. Despite the local character of the hyperfine interaction, single nuclear spin manipulation is hard to achieve, an inconvenience which can be overcome by using instead nuclear spin clusters⁷. For GaAs quantum wells and quantum dots the nuclear spin coherence time can be as long as a second^{8,9}, much longer than the electron spin coherence time, of the order of 100 ns (Ref. 10).

Control over the nuclear spin dynamics in semiconductor nanostructures is realized by various methods. Control of collective excitations^{11,12} can modify the enhanced nuclear spin relaxation times in a GaAs quantum well (QW). Adjacent ferromagnetic layers can “imprint” nuclear spin¹³ in *n*-type GaAs QW’s. A flexible method of nuclear spin manipulation, using gate voltages to electrically address a wide distribution of polarized nuclei within an AlGaAs parabolic quantum well (PQW), was recently demonstrated¹⁴. Optically injected spin polarized electrons transfer their spin polarization to the nuclear population via dynamic nuclear polarization (DNP)¹⁵, resulting in a position dependent nuclear polarization within the PQW. Gate voltages are then used to shift the electron population and thus produce polarized nuclei with different probabilities at various positions in the PQW. The position dependent nuclear polarization was measured by time resolved Faraday rotation (TRFR) experiments, which showed¹⁴ that a 8 nm wide distribution of polarized nuclei can be manipulated electrically over a range of 20 nm.

Here we derive general formulas describing the nuclear polarization, and resulting nuclear dipolar fields,

achieved dynamically in low dimensional semiconductor nanostructures due to the hyperfine interaction between electronic and nuclear spins. Just as was found for nuclear and electron relaxation times⁹, the central physical quantity determining the nuclear polarization is the electronic local density of states (ELDOS) at the nuclear position. The position dependence of the induced nuclear polarization in semiconductor nanostructures is shown to be a function of the initial polarization of the electronic population and various nuclear interactions which lead to nuclear spin relaxation. We calculate how the nuclear polarization within the semiconductor nanostructure can be manipulated with electric fields by changing the ELDOS at particular locations. Our results are relevant for nuclear magnetic resonance (NMR) and TRFR experiments in semiconductor nanostructures^{16–18}. For AlGaAs PQW’s we propose an experimental setup where the efficiency of optical DNP will be enhanced by the proper insertion of a δ -doped layer of different nuclei at a specific position. Calculations of the induced nuclear polarization also allow us to predict the nuclear magnetic resonance shift in semiconductor nanostructures.

The paper is organized as follows. In the next Section we present a theoretical derivation of DNP in samples with reduced dimensionality. Section III presents numerical estimations for the induced nuclear spin polarization and the resulting dipolar nuclear magnetic fields for an AlGaAs PQW. Section IV gives our conclusions.

II. DYNAMICAL NUCLEAR POLARIZATION

Dynamical nuclear polarization was theoretically described by Overhauser¹⁵ in bulk metallic samples. The interaction between nuclear and electronic spins leads to an enhanced nuclear spin polarization which can be measured in NMR and TRFR experiments. For semiconductor bulk materials such as GaAs, the DNP effect can be enhanced via optical techniques^{19,20}. The same optical pumping technique was successfully used to polarized nuclei in quasi two-dimensional semiconductor

heterostructures^{8,21}. In this Section we investigate theoretically DNP in samples with reduced dimensionality such as quantum wells and quantum dots (QD).

The hyperfine interaction between electronic and nuclear spins is described by the Hamiltonian

$$H_n = \frac{8\pi}{3} \beta_e \beta_n (\vec{\sigma}_n \cdot \vec{\sigma}_e) \delta(\mathbf{r} - \mathbf{r}_n), \quad (1)$$

where n labels the nuclei, β_n and β_e are the nuclear and electron magnetic moments, $\vec{\sigma}_n$ and $\vec{\sigma}_e$ are the Pauli spin operators for the nucleus and electron, $\mathbf{r} - \mathbf{r}_n$ represents the relative distance between the nuclear and electronic spins, and $\delta(\mathbf{r})$ is the Dirac delta function. The Hamiltonian describes a flip-flop process for both electronic and nuclear spins in which the energy and the total angular momentum are conserved. We consider the interaction to be weak, so we can use perturbation theory to describe its effects. To understand the dynamics of the electronic and nuclear spins governed by the hyperfine interaction we consider the system to be in an external magnetic field, B_0 , which partially orients the spins. We assume dephasing of electronic orbital information on timescales much faster (~ 100 fs) than either the precession of electron spins in momentum-dependent effective magnetic fields²² or nuclear decoherence times; this permits us to neglect the momentum-dependent spin splitting of electronic states from the spin-orbit interaction²². The electronic spin polarization is assumed the same everywhere, described by the spin-up and spin-down populations N_+ (parallel to the applied field) and N_- (antiparallel to the applied field), respectively. On the other hand, the nuclear system will develop a position dependent polarization described by $M_m(\mathbf{r}_n)$, $m = I, I-1, \dots, -I$, where I is the nuclear spin quantum number. The hyperfine interaction will act to relax both the electronic and the nuclear spins, according to the following two equations²³

$$\frac{dD}{dt} = \frac{D_0 - D}{T_{1e}} + \sum_n \frac{\Delta_0(\mathbf{r}_n) - \Delta(\mathbf{r}_n)}{T_{1n}(\mathbf{r})} \quad (2)$$

and

$$\frac{dD}{dt} = -\frac{2I(I+1)(2I+1)}{3} \sum_n \frac{d\Delta(\mathbf{r}_n)}{dt}. \quad (3)$$

Here $D = N_+ - N_-$, $\Delta(\mathbf{r}_n) = M_{m+1}(\mathbf{r}_n) - M_m(\mathbf{r}_n)$, and D_0 and $\Delta_0(\mathbf{r}_n)$ are their thermal equilibrium values. The electronic and nuclear spin relaxation times are given by (see Refs. 9,23)

$$T_{1e}^{-1} = \frac{1}{V} \sum_n \frac{1024\pi^3 \beta_e^2 \beta_n^2 \int d\varepsilon A_e^2(\mathbf{r}_n, \varepsilon) f'_{FD}(\varepsilon)}{9\hbar(2I+1) \int d\mathbf{r} d\varepsilon A_e(\mathbf{r}, \varepsilon) f'_{FD}(\varepsilon)} \quad (4)$$

and

$$T_{1n}^{-1}(\mathbf{r}_n) = \frac{512\pi^3 \beta_e^2 \beta_n^2 k_B T \int d\varepsilon A_e^2(\mathbf{r}_n, \varepsilon) f'_{FD}(\varepsilon)}{3\hbar I(I+1)(2I+1)}, \quad (5)$$

where $A_e(\mathbf{r}_n, \varepsilon)$ represents the ELDOS, T is the temperature, and $f_{FD}(\varepsilon)$ the Fermi-Dirac distribution function.

The ELDOS at the nuclear position \mathbf{r}_n is

$$A_e(\mathbf{r}_n, \varepsilon) = \sum_l |\psi_l(\mathbf{r}_n)|^2 \delta(\varepsilon - E_l), \quad (6)$$

where l labels the state, E_l its energy, and $\psi_l(\mathbf{r}_n)$ its wavefunction at the n 'th nucleus. Equations (2) and (3) can be combined to obtain a general equation for the nuclear spin dynamics

$$\frac{d\Delta(\mathbf{r}_n)}{dt} = \frac{\Delta_0(\mathbf{r}_n) - \Delta(\mathbf{r}_n)}{T_{1n}(\mathbf{r}_n)} + \frac{1}{(2I+1)k_B T \tilde{N}} \frac{D_0 - D}{T_{1n}(\mathbf{r}_n)}, \quad (7)$$

where $\tilde{N} = \int d\mathbf{r} d\varepsilon A_e(\mathbf{r}, \varepsilon) f'_{FD}(\varepsilon)$. The above equation describes the nuclear spin dynamics due to the hyperfine interaction. Additionally, the nuclei will relax through other mechanisms as a result of interactions with phonons, impurities, electrons, and other nuclei. Such interactions should be included in any equation for the nuclear spin dynamics, and they can be included by replacing $1/T_{1n}(\mathbf{r}_n)$ with $1/T_{1n}(\mathbf{r}_n) + 1/T'_n$ in the first term on the right hand side (rhs) of Eq (7). Here T'_n represents the nuclear spin relaxation time due to additional relaxation mechanisms. Note that such a replacement is not appropriate for the second term in the rhs of Eq. (7), as this term originates from the hyperfine interaction alone.

Equation (7) also assumes that nuclear spin diffusion can be neglected. The nature of the sample determines whether or not nuclear spin diffusion can be neglected. Paget²⁴ showed that in bulk GaAs diffusion is very important, and leads to an uniform polarization of the nuclei across the sample. To describe diffusion the equation for the time and position dependence of the nuclear spin polarization has to be modified by adding a diffusive term. However, often nuclear spin diffusion appears negligible for low dimensional samples such as QW and QD^{14,25}. In the following we will discuss the consequences of the DNP effect in the absence of nuclear spin diffusion. Such an assumption should work well for PQW's, the system for which we will report specific results^{9,14}.

In DNP, spin polarized electrons created by absorption of polarized light or electrical injection²⁵ will transfer their polarization to the nuclei via the hyperfine interaction. We assume that the electronic polarization, D , is kept constant by continual resupply of spin polarized electrons. This would naturally be the case for DC electrical spin injection. For pulsed optical pumping, however, the spin-polarized electron population will vary on timescales corresponding to the time between pulses (~ 13 ns). Here we rely on the vastly greater timescales of the nuclei — as the response times of the nuclei (T_{1n}) are orders of magnitude greater than 13 ns, the nuclei see an effective constant average electron spin polarization. Under these conditions the last term in Eq. (7) is independent of time and the time-dependent nuclear

polarization is

$$\Delta(\mathbf{r}_n, t) = \Delta_0 + \Delta_{ind}(\mathbf{r}_n) \left\{ 1 - \exp \left[-t \left(\frac{1}{T_{1n}(\mathbf{r}_n)} + \frac{1}{T'_n} \right) \right] \right\}, \quad (8)$$

where

$$\Delta_{ind}(\mathbf{r}_n) = \frac{1}{(2I+1) k_B T \tilde{N}} \frac{T'_n}{T_{1n}(\mathbf{r}_n) + T'_n} (D_0 - D) \quad (9)$$

represents the induced nuclear polarization due to the hyperfine interaction. In general the nuclear polarization due to external magnetic fields, Δ_0 , is about 1%, suggesting that the large nuclear polarization originates from the hyperfine interaction.

Two different time regimes can be identified in Eq. (8). First, in the initial stages of the DNP process ($t \ll T_{eff}$; with $T_{eff}^{-1} = T_{1n}^{-1} + T_n'^{-1}$), the nonequilibrium nuclear system magnetization can be approximated as

$$\Delta(\mathbf{r}_n, t) \approx \Delta_{ind}(\mathbf{r}_n) \frac{t}{T_{eff}}. \quad (10)$$

In general, at low temperatures where the DNP process is efficient, the relaxation mechanism due to the hyperfine interaction is the dominant one, making T_{1n} shorter than T'_n . Accordingly, in the initial stage of the DNP process, $\Delta(\mathbf{r}_n, t) \propto |\psi_l(\mathbf{r}_n)|^4 t$ (Ref. 9). On the other hand, in the second regime of the DNP process for $t \gg T_{eff}$, the induced nuclear spin polarization from the hyperfine interaction will saturate at

$$\Delta(\mathbf{r}_n, t) = \Delta_0 + \frac{1}{(2I+1) k_B T \tilde{N}} \frac{T'_n}{T_{1n}(\mathbf{r}_n) + T'_n} (D_0 - D). \quad (11)$$

III. NUCLEAR SPIN POLARIZATION AND DIPOLAR MAGNETIC FIELDS

Large non-equilibrium nuclear polarizations produce real magnetic fields that act both on the nuclear and on the electronic spins. A significant effect of these fields is the shift of resonant frequencies in magnetic resonance experiments associated with nuclei or electrons. Below we address primarily the effects of DNP on NMR experiments; their effect on TRFR experiments will be reported elsewhere²⁶.

We determine the nuclear magnetic fields from the non-equilibrium occupation of the different states of the nuclear spin due to the DNP process, and we neglect the equilibrium polarization Δ_0 from the static magnetic field. The induced nuclear spin polarization,

$$\mathcal{P} = \frac{\sum_m m M_m}{I \sum_m M_m}. \quad (12)$$

For nanostructured materials \mathcal{P} will depend on position, as nuclei in different regions of the sample overlap differently with the electronic wavefunctions. Also, the time-dependence of the DNP process will cause the nuclear

spin polarization to depend on time as well. The induced nuclear magnetization is

$$\mathcal{M}_{ind}(\mathbf{r}_n) = \sum_m m M_m(\mathbf{r}_n). \quad (13)$$

The observable physical quantity in NMR experiments, however, is the nuclear magnetic field produced by this nonequilibrium magnetization. The position-dependent induced nuclear magnetic field can be calculated for *layered* structures by dividing the structure into thin slabs stacked in the growth direction and labeled by z_n , and assuming that the nuclei in each slab have uniform magnetization. Nuclei in different slabs can have different magnetization due to the potential dependence of the nuclear relaxation time on the growth direction⁹ due to a non-uniform ELDOS. The dipolar field from the nuclei, if they are polarized perpendicular to the growth direction, is

$$B_{ind}(\mathbf{r}_n) = \mu_0 \mu_n \mathcal{M}_{ind}(\mathbf{r}_n), \quad (14)$$

where μ_0 represents the vacuum permeability and μ_n the nuclear magneton. This magnetic field will act both on the nuclei and the electrons, and for nuclei the effect can be measured as a shift in the resonance frequency in an NMR experiment. This effect is similar to the Knight shift²⁷, and can be characterized by

$$\Delta\nu(\mathbf{r}_n) = g_n \mu_n B_{ind}(\mathbf{r}_n), \quad (15)$$

where g_n is the nuclear g-factor. For low dimensional nanostructures the shift will depend on position. The total nuclear magnetic moment of the sample is

$$M = \int d\mathbf{r}_n \mu_n \mathcal{M}_{ind}(\mathbf{r}_n). \quad (16)$$

For a PQW structure the system's dispersion relations are quasi-two dimensional, and the total electronic wavefunction is a product between an envelope function, $\phi(z)$, and a Bloch function, $u(\mathbf{r})$,

$$\psi_{j\mathbf{K}}(\mathbf{r}_n) = \exp[i\mathbf{K} \cdot \mathbf{R}] \phi_j(z) u(\mathbf{r}_n). \quad (17)$$

Based on this assumption the ELDOS is

$$A_e(\mathbf{r}_n, \varepsilon) = \sum_j |\phi_j(\mathbf{z}_n)|^2 N_{2D} \Theta(\varepsilon - E_{j(\mathbf{K}=0)}), \quad (18)$$

where N_{2D} is the density of states for a two-dimensional electron gas and $\Theta(z)$ is the Heavyside step function. In the following we will consider an $\text{Al}_x\text{Ga}_{1-x}\text{As}$ PQW ($L = 1000 \text{ \AA}$) with $x=0.07$ in the center of the structure confined within two 100 \AA $\text{Al}_{0.4}\text{Ga}_{0.6}\text{As}$ barriers. For this structure the value of the Bloch function at Ga nuclei was already extracted in Ref. 9 and the envelope functions will be evaluated using a 14-band $\mathbf{k} \cdot \mathbf{p}$ calculation²⁸. For all calculations we consider only the first electronic conduction subband occupied and the electron spin polarization, $D = 100\%$, much greater than the thermodynamic equilibrium one, D_0 . The additional nuclear spin

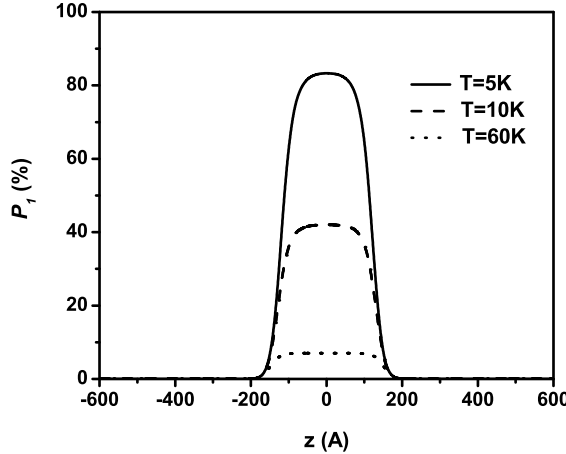


FIG. 1: The growth-direction position dependence of the saturated induced nuclear spin polarization in the AlGaAs PQW for $T'_n = 600$ s and different temperatures (full line— $T = 5$ K, dash line— $T = 10$ K, and dash-dot line— $T = 60$ K).

relaxation time, $T'_n = 600$ s, and is considered to be temperature independent²⁹.

Figure 1 presents a quantitative plot of the saturated induced nuclear spin polarization, $P_{sat}(\mathbf{r}_n)$ as a function of position in the AlGaAs PQW at different temperatures. For fully polarized electrons ($D = 100\%$) the induced nuclear spin polarization in the center of the PQW can be as high as 80%, decreasing drastically on the sides of the sample. The nuclear spin polarization also decreases as the temperature increases, making the DNP process effective only at low temperatures. If higher electronic subbands were considered, the position dependence of the saturated nuclear spin polarization would change accordingly.

Figure 2 presents a quantitative plot of the induced nuclear magnetic field $B_{ind}(\mathbf{r}_n, t)$ as a function of time and position across the AlGaAs PQW for the same situation as in Fig. 1. The strong confinement, even of this shallow PQW structure, is reflected in the large induced nuclear magnetic field at the center. The total response of the sample in NMR experiments will be mainly due to the central nuclei of the sample, suggesting that a more effective DNP can be realized by the insertion of active NMR nuclei at a particular growth-direction position in the sample. For higher conduction subband occupancy the profile of the induced nuclear field will change accordingly, as a result of a different position dependent nuclear spin relaxation time due to the hyperfine interaction⁹.

In Fig. 3 we present the position dependence of the saturated induced nuclear magnetic field for different values of the additional nuclear spin relaxation time, T'_n , considering only the first conduction subband occupied. As seen in Fig. 3(a) the full width at half maximum (FWHM) of the induced nuclear magnetic field is strongly dependent on the additional relaxation mechanisms involving nuclear spins. At low temperatures,

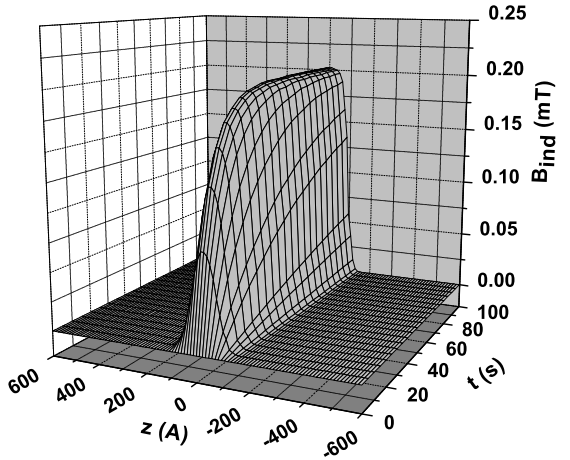


FIG. 2: The time and position dependence of the induced nuclear dipolar magnetic field in the AlGaAs PQW for $T'_n = 600$ s.

where most of our calculations are performed, the dominant nuclear spin relaxation mechanism is the hyperfine interaction, and the measurement of additional nuclear spin relaxation times is very difficult. Fig 3 (b) presents the saturated induced nuclear magnetic field for $T'_n = 600$ s in the presence of and in the absence of an applied electric field along the growth direction for the PQW. The control is based on the manipulation of the ELDOS. Our calculation suggests the possibility of further controlling and manipulating the nuclear spin distribution in AlGaAs PQW. When a δ -doped layer of active nuclei is inserted within the PQW, the initial nuclear polarization of the nuclei in the layer can be directly controlled by electric fields. A different way to electrically control the induced position dependent nuclear field would be to gate the PQW and control the hyperfine nuclear spin relaxation time through the electronic subband occupancy^{9,23}. Different shapes and different position dependences of the induced nuclear field are expected in this case.

Fig 4(a) presents the calculated nuclear resonance shift for the AlGaAs PQW for different conduction subband occupancy at $T = 5$ K. This situation is relevant for a δ -doped layer of active nuclei, and the nuclear resonance shift can reach 8.5 kHz. Moreover, for a δ -doped layer, the resonance shift is fully controllable with electric fields, both when the field is used as a control over the electron confinement in the PQW or when the field is used as a source of subband occupancy in the PQW. Fig 4(b) shows the total nuclear magnetic moment as a function of the electron density for different temperatures. As the electron density increases, the number of occupied conduction subbands will increase, and accordingly the nuclear magnetic moment of the well will increase quasi-stepwise. For the considered PQW the energy difference between the minimum of two consecutive conduction sub-

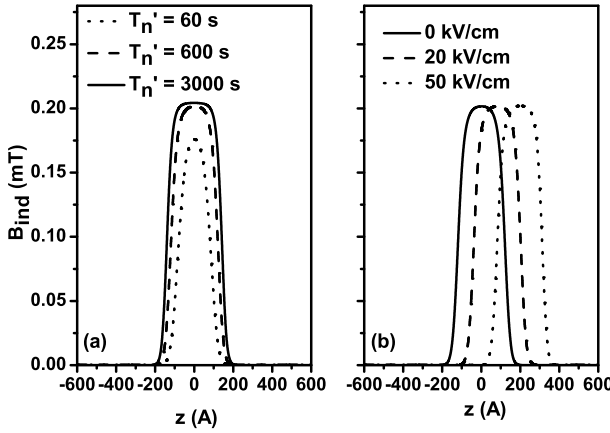


FIG. 3: (a) The saturation value of the induced nuclear polarization in the AlGaAs PQW for different values of the additional nuclear relaxation time (full line: $T'_n = 3000$ s, dashed line: $T'_n = 600$ s, and dotted line: $T'_n = 60$ s). (b) The saturation value of the induced nuclear polarization in the AlGaAs PQW for $T'_n = 600$ s at different values of the applied electric field (full line: $F = 0$ kV/cm, dashed line: $F = 20$ kV/cm, and dotted line: $F = 50$ kV/cm).

bands is about $\Delta E = 15$ meV, meaning that at $T = 30$ K (dotted line) thermal smearing of the Fermi function will suppress the stepwise shape of the total nuclear magnetic moment. For PQW's with a greater difference ΔE the stepwise shape will persist even at higher temperatures. The total nuclear magnetic moment for a fixed electronic density depends on temperature, as T_{1n} and T'_n have different temperature dependencies (in Fig. 4 (b) we considered $T_{1n} \sim T$ and $T'_n \sim \text{const.}^{9,29}$).

IV. CONCLUSIONS

The DNP process is of considerable interest for samples with reduced dimensionality as it represents a path for highly efficient NMR and TRFR measurements. As a result of DNP, nuclei will produce effective magnetic fields which in turn will act both on the nuclear and electronic populations. The effects of those magnetic fields should be observable in NMR and TRFR experiments as shifts in the resonant frequencies. Usually, as a result of the hyperfine interaction there will be at least two types of induced nuclear magnetic fields, a hyperfine nuclear magnetic field and a dipolar magnetic field. The hyperfine magnetic field acting on the nuclear population is an effective magnetic field induced by the polarized electronic population. There will be also a hyperfine field created by the polarized nuclei acting on the electrons. Such hyperfine fields will induce a Knight shift in the nuclear resonant frequencies, and an Overhauser shift in the electronic resonant frequencies, respectively. On the other hand, the dipolar magnetic field is a real magnetic

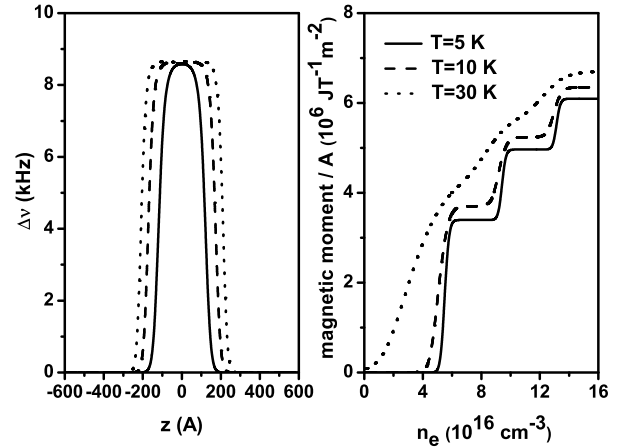


FIG. 4: (a) The nuclear resonance frequency shift as function of position in the PQW for different conduction subband occupancy at $T=5$ K (full line: single subband occupancy, dashed line: double subband occupancy, and dotted line: triple subband occupancy). (b) Total nuclear induced magnetic moment as function of the electron density for different temperatures (full line: $T=5$ K, dashed line: $T=10$ K, and dotted line: $T=30$ K).

field created as a result of nuclear spin polarization. The dipolar nuclear magnetic field will be responsible for an additional shift in the resonant frequencies of both nuclear and electronic systems similar to Knight and Overhauser shifts, respectively.

For general low dimensional systems we described the dynamics of the nuclear spins for optical pumping of the electronic population. The resulting nuclear spin polarization is both time and position dependent. In the initial stage of the polarization process, the induced nuclear polarization is linearly dependent on time. For longer times the nuclear spin polarization saturates and is time independent. The position dependence of the induced nuclear spin polarization is a function of the electronic confinement across the system, and of various relaxation mechanisms acting on the nuclear spin. Consequently, the resonance shift induced by such a field will be position dependent. Different experimental setups will record different resonance shifts. For example, if the sample is grown such that in the central region we have a δ -doped layer of a different nuclei than the host nuclei, the resonance shift for such a layer will strongly depend on its position across the well. On the other hand, in different experiments it may be that whole magnetic moment of the sample is recorded.

As a specific example we calculated the effects of the DNP process for an AlGaAs PQW. The nuclear spin polarization can be as high as 80% at $T = 5$ K for an initial electronic spin polarization of 100%. The nuclear spin polarization is concentrated in the central regions of the PQW and depends also on temperature, being strongly reduced as the temperature increases. The DNP effect

provides the potential to manipulate nuclear spins in semiconductor nanostructures, making the nuclear spins an important candidate for new electronic devices. The particular geometry of the PQW permits a sensitive con-

trol of nuclear spins with small electric fields.

We would like to acknowledge D. D. Awschalom and M. Poggio for helpful discussions. Our work was supported by DARPA/ARO DAAD19-01-1-0490.

^{*} Permanent address: Department of Theoretical Physics, “Babeş-Bolyai” University of Cluj, 3400 Cluj, Romania.

¹ *Semiconductor Spintronics and Quantum Computation*, edited by D. D. Awschalom, N. Samarth, and D. Loss (Springer, New York, 2002).

² S. A. Wolf, D. D. Awschalom, R. A. Buhrman, J. M. Daughton, S. von Molnár, M. L. Roukes, A. Y. Chtchelkina, and D. M. Treger, *Science* **294**, 1488 (2001).

³ D. Loss and D. P. DiVincenzo, *Phys. Rev. A* **57**, 120 (1998).

⁴ B.E. Kane, *Nature (London)* **415**, 281 (2002).

⁵ J.M. Taylor, C.M. Marcus, and M.D. Lukin, *Phys. Rev. Lett.*, **90**, 206803 (2003).

⁶ N.A. Gershenfeld and I.L. Chuang, *Science* **275**, 350 (1997).

⁷ F. Meier, J. Levy, and D. Loss, *Phys. Rev. B* **68**, 134417 (2003).

⁸ S. E. Barrett, R. Tycko, L. N. Pfeiffer, and K. W. West, *Phys. Rev. Lett* **72**, 1368 (1994).

⁹ I. Tifrea and M.E. Flatté, *Phys. Rev. Lett.* **90**, 237601 (2003).

¹⁰ J. M. Kikkawa and D. D. Awschalom, *Phys. Rev. Lett.* **80**, 4313 (1998).

¹¹ J.H. Smet, R.A. Deutschmann, F. Ertl, W. Wegscheider, G. Abstreiter, and K. von Klitzing, *Science* **415**, 281 (2002).

¹² W. Desrat, D.K. Maude, M. Potemski, J.C. Portal, Z. R. Wasilewski, and G. Hill, *Phys. Rev. Lett.* **88**, 256807 (2002).

¹³ R.K. Kawakami, Y. Kato, M. Hanson, I. Malajovich, J.M. Stephens, E. Johnson-Halperin, G. Salis, A.C. Gossard, and D.D. Awschalom, *Science* **294**, 131 (2001).

¹⁴ M. Poggio, G.M. Steeves, R.C. Myers, Y. Kato, A.C. Gossard, and D.D. Awschalom, *Phys. Rev. Lett.* **91**, 207602 (2003).

¹⁵ A.W. Overhauser, *Phys. Rev.* **92**, 411 (1953).

¹⁶ J.A. Marohn, P.J. Carson, J.Y. Hwang, M.A. Miller, D.N. Shykind, and D.P. Weitekamp, *Phys. Rev. Lett.* **75**, 1364 (1995).

¹⁷ A. Malinowski and R.T. Harley, *Solid State Commun.* **114**, 419 (2000).

¹⁸ G. Salis, D.D. Awschalom, Y. Ohno, and H. Ohno, *Phys. Rev. B* **64**, 195304 (2001).

¹⁹ D. Paget, G. Lampel, B. Sapoval, and V.I. Safarov, *Phys. Rev. B* **15**, 5780 (1977).

²⁰ J. M. Kikkawa and D. D. Awschalom, *Science* **287**, 473 (2000).

²¹ A. Berg, M. Dobers, R.R. Gerhardts, and K. von Klitzing, *Phys. Rev. Lett.* **64**, 2563 (1990).

²² G. Dresselhaus, *Phys. Rev.* **100**, 580 (1955).

²³ I. Tifrea and M.E. Flatté, *Phys. Rev. B* **69**, 115305 (2004).

²⁴ D. Paget, *Phys. Rev. B* **25**, 4444 (1982).

²⁵ J. Strand, B. D. Schultz, A. F. Isakovic, C. J. Palmstrom, and P. A. Crowell, *Phys. Rev. Lett.* **91**, 036602 (2003).

²⁶ I. Tifrea, M. Poggio, M.E. Flatté, and D.D. Awschalom, unpublished.

²⁷ C.P. Slichter, *Principles of Magnetic Resonance*, (Springer, New York, 1990).

²⁸ W.H. Lau, J.T. Olesberg, and M.E. Flatté, cond-mat/0406201, (unpublished).

²⁹ J.A. McNeil and W.G. Clark, *Phys. Rev. B* **13**, 4705 (1976).